Temperature dependence of the dynamic susceptibility of nickel

J. W. Lynn*† and H. A. Mook
Solid State Division, Oak Ridge National Laboratory, Oak Ridge, Tennessee 37830
(Received 7 April 1980)

The coherent magnetic inelastic scattering of neutrons has been used to measure the dynamic susceptibility $\chi(\vec{q}, \omega)$ of nickel from low temperatures to well above the ferromagnetic transition temperature. As the temperature approaches T_C from below, the linewidths of the spin waves are found to broaden, and in the small wave-vector region the scattering is in general agreement with dynamic scaling theory. At larger wave vectors, however, we find that the observed scattering can be more naturally described in terms of spin-wave-like excitations whose widths ΔE remain less than the excitation energies E ($\Delta E/E < 1$) for $T > T_C$. The "dispersion relation" for these spin waves is only moderately renormalized up to T_C and then remains constant as the temperature is raised further up to at least twice T_C, while the widths continue to broaden slowly above T_C. The overall magnitude of the susceptibility decreases with increasing temperatures, but the abrupt decrease of $\chi(\vec{q}, \omega)$ at high energies, interpreted as the intersection of the collective excitation spectrum with the Stoner continuum of single-particle excitations, is found to be insensitive to the temperature. These results are compared and contrasted with the recent results for iron.

I. INTRODUCTION

It is now generally established that the low-temperature electronic and magnetic properties of the $3d$ ferromagnetic metals can be understood in terms of their band structures. In particular, the neutron scattering results for iron and nickel at low temperatures are best described by calculations of the generalized susceptibility $\chi(\vec{q}, \omega)$ based on band structures in which the electron correlations are handled as accurately as possible.[1–3] A proper incorporation of these electron correlations is of course crucial to obtaining an accurate description of the collective excitations of the magnetic system, and the overall agreement between theory and experiment gives us confidence that this band picture of the excitation spectrum is generally correct. Extending the theory to include the general effects of temperature presents considerable complications. The nature of the band structure and the electron correlations at elevated temperatures is not yet fully illuminated, although considerable theoretical progress has been made recently.[4–10]

The neutron scattering technique can provide detailed microscopic information about a magnetic system, and a great deal of information concerning the spin dynamics of Ni at elevated temperatures has already been obtained. The long-wavelength spin dynamics have been studied in detail by Minkiewicz *et al.*[11] using the triple-axis technique. They found that in the small-wave-vector region the spin-wave dispersion relation renormalizes according to a power law of the reduced temperature as T_C is approached, and the spin waves become overdamped just below T_C. Temperature-dependent measurements of $\chi(\vec{q}, \omega)$ have also been made by Lowde and Windsor,[12] and their results have served as a first step in an overall determination of $\chi(\vec{q}, \omega)$ for nickel. Our results have substantiated many of the general features of the Lowde and Windsor investigation while adding greatly to the accuracy and resolution of the measurements. At high temperatures we find features of $\chi(\vec{q}, \omega)$, particularly the relatively well-defined spin-wave mode and the abrupt decrease of the intensity at high energies, which were not observable in their data.

At room temperature the spin-wave part of $\chi(\vec{q}, \omega)$ has been measured in detail. However, since the magnon dispersion relations in the $3d$ metals are very steep, at larger wave vectors the magnon energies become rather high for standard neutron scattering techniques to measure. Minkiewicz *et al.*[11] measured a portion of the dispersion relation and found that the spin waves were isotropic in $\vec{q}$ up to the highest energy transfers they measured (~ 70 meV). Mook, Nicklow, and collaborators[13] extended the room-temperature spin-wave measurements for nickel to higher energies, and found that the spin-wave intensities were roughly constant until about 100 meV, and then dropped suddenly by more than an order of magnitude, becoming unobservable. The falloff in intensity occurred at different energies in different symmetry directions in the crystal, and was interpreted as the intersection of the spin-wave modes with the Stoner continuum of excitations. More recent measurements[14] show that the acoustic

spin wave runs into an optical spin wave in the [100] direction. Above this intersection well-defined spin waves are still observable but with reduced intensity. No such optical mode has been observed in the [111] direction, however, and the spin waves dying out appears to be the result of entering the Stoner continuum. Similar results have been obtained for iron,[15,16] and this interpretation has been substantiated by detailed calculations[1-3] of $\chi(\vec{q}, \omega)$.

With increasing temperature it was expected that the splitting between the spin-up and spin-down electron energy bands would decrease and hence the region of Stoner excitations which controls the spin-wave lifetimes would also decrease in energy. This would then bring the spin-wave–Stoner intersection into a more favorable energy region to study with neutrons, and consequently this could be investigated in greater detail. However, it was found[17] that the energy at which the spin-wave mode disappeared was insensitive to the temperature, and that in addition, above the ferromagnetic ordering temperature, relatively well-defined propagating excitations were found outside the small-wave vector–low-energy region. Similar behavior was found[16] for the magnetic response of Fe at elevated temperatures. The present study reports the full details of our investigations into the temperature dependence of the dynamic susceptibility of nickel.

II. EXPERIMENTAL APPARATUS AND PROCEDURES

The majority of the measurements were taken on the HB-3 triple-axis neutron spectrometer installed at the High Flux Isotope Reactor (HFIR) at the Oak Ridge National Laboratory. The sample was a 123-g single crystal of the isotope ^{60}Ni. The use of this isotope greatly reduced unwanted nuclear cross sections and thus improved the magnetic signal-to-noise ratio. Additional high-resolution measurements were taken on the HB-4A triple-axis neutron spectrometer also at HFIR. The triple-axis technique has been discussed at length in the literature,[18] and with particular regard to the present measurements many of the details of the data analysis have already been presented in Refs. 15 and 16 and will therefore not be repeated here. We will refer to these data analysis techniques as appropriate when the data are presented. There are, however, a few additional details of particular relevance to the spin-wave intensity measurements at high energies which should be mentioned.

We first briefly review the three basic requirements that dictate the mode of operation of the neutron spectrometer to measure the spin-wave scattering from iron and nickel. Since the spin-wave excitations in iron and nickel extend to high energies (compared to kT), all the measurements have been taken with the incident energy E_0 greater than the scattered energy E', so that the neutrons create spin waves in the crystal. This is necessary because the Bose thermal factor is much less than one for the high-energy spin waves. The second consideration arises because the spin-wave dispersion relations in the $3d$ metals are very steep. This necessitates measuring the higher-energy spin waves by fixing the energies of the incident and scattered neutrons that the spectrometer transmits and by varying the wave-vector transfer $\vec{K}$, which is called a "constant-E" scan. This type of scan will cut directly across the dispersion surface, giving a sharp peak in the scan. The more familiar "constant-$\vec{Q}$" scan (or "constant-$\vec{K}$" scan) would almost parallel the spin-wave dispersion surface. The resolution ellipsoid would then "drag" along the dispersion surface over a large energy range, giving a very broad distribution of scattered intensity. Finally, although the elementary excitation spectrum in a periodic lattice is itself periodic [so that $\hbar\omega(q) = \hbar\omega(\vec{q} + \vec{\tau})$, where $\vec{\tau}$ is any reciprocal-lattice vector], the neutron scattering intensity does not have this same periodicity. An important intensity consideration is related to the magnetic form factor $F(\vec{K})$, which is the Fourier transformation of the magnetization density in the unit cell. To maximize the scattered intensity, $\vec{K}$ must be kept as small as practical. This has important consequences when measuring the high-energy spin waves, as demonstrated in Fig. 1. If we want to measure the scattering at a large energy transfer, then there must be a large difference in the lengths of the initial and final wave vectors $\vec{k}_0$ and $\vec{k}'$. However, in order to keep $\vec{K}$ ($\vec{K} = \vec{\tau} + \vec{q}$) reasonably small and still satisfy the conservation of energy and momentum, $\vec{k}'$ must be fairly large also. Thus very high incident neutron energies must be used. For the measurement of spin waves ~ 100 meV, incident neutron energies ~ 200 meV have to be used. At these energies the flux of neutrons from the reactor is greatly reduced, so that the required counting times for the measurement of these spin waves are very long. Fortunately, because

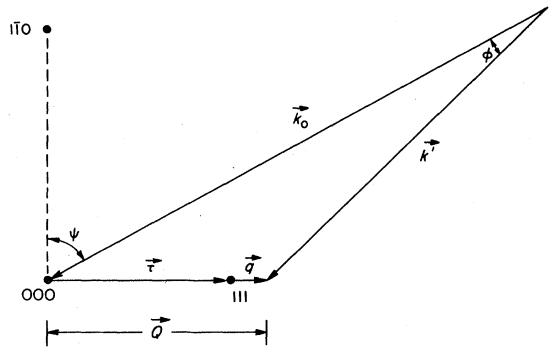

FIG. 1. Typical scattering diagram for the measurement of a high-energy spin wave.

of the design characteristics of the HFIR, the entire energy spectrum of the neutrons is shifted to somewhat higher energies compared with many other research reactors, so that the flux of high-energy neutrons onto the sample is enhanced. Without the high flux of high-energy neutrons as well as the large single-crystal samples grown from isotopes which are particularly favorable for measuring the magnetic scattering, these measurements of the spin-wave intensities at high energies in nickel (and iron) would not have been possible.

In addition to the experimental details given in Refs. 13–17, there are a number of other experimental factors which may influence the spin-wave intensity measurements, particularly at high energies, which we would like to discuss. When the monochromating and analyzing crystals are set to reflect a wavelength λ, they may also reflect higher-order wavelengths (recall that Bragg's law is $n\lambda = 2d\sin\theta$). Thus when the spectrometer is set to measure $(\vec{k}_0, \vec{k}', E_0, E')$ it may also transmit $(\vec{k}_0, 2\vec{k}', E_0, 4E')$, $(2\vec{k}_0, \vec{k}', 4E_0, E')$, etc. These extra processes can give rise to "spurious" peaks, i.e., to peaks which are not expected due to the primary scattering configuration. These peaks may occur in scans of any energy transfer, but they can be particularly bothersome for the high-energy measurements where the magnetic scattering is small and the resolution is coarse. However, the positions of these peaks can be calculated and often avoided, and the cross section can be measured under different experimental arrangements and checked for consistency of results. This is time consuming, though, and these spurious-peak processes are one of the major problems with triple-axis spectrometers. A second low-efficiency detector has also been placed between the sample and analyzer to detect Bragg scatterings from the sample, which can also give rise to spurious peaks in the scans, and to monitor the general background level.

Another potential problem is associated with multiple Bragg reflections in the monochromator crystal. The intensity of these multiple reflections is generally much smaller than that of the primary scattered beam, but at high incident energies multiple reflections may become significant. In addition to giving rise to possible "spurious" peaks, this could introduce additional counts into the incident beam monitor and hence the spin-wave scattering cross section (per unit monitor interval) would appear to be reduced. Careful checks have been made to minimize these effects.

For high incident energies incoherent scattering processes occurring in the monochromator may also contribute a significant number of neutrons to the beam incident onto the sample. This may be easily corrected for by setting the monochromator crystal off the Bragg peak and counting the number of neutrons incoherently scattered. At the highest energies used the incoherent scattering amounted to no more than 5% of the incident flux, and the spin-wave intensities have been corrected for this effect.

Finally, Bragg reflections may occur in the sample, and "rob" the incident beam of neutrons inside the sample. This effect may become more important for the higher energies (shorter wavelengths) since more Bragg reflections can occur. To check the magnitude of this effect, the beam transmitted through the nickel crystal was monitored as a function of energy. No appreciable effect was observed, and no corrections have been made for it.

III. RESULTS

The ferromagnetic transition temperature for Ni is 631 K, so that room temperature is practically half the Curie temperature. Consequently, in addition to taking data above room temperature, measurements were also carried out at 4.2 K in a liquid-helium cryostat.

The spin-wave dispersion relations, as well as the intrinsic linewidths at elevated temperatures, were found to be isotropic in $\vec{q}$ over the entire temperature (4.2 → 1260 K) and energy ($\lesssim 100$ meV) range explored. We have therefore concentrated our measurements in the [111] direction. The dispersion relation as measured in constant-E scans is shown in Fig. 2 for $0 < T/T_C \leq 2$. As the temperature is increased to T_C, the spin waves are seen to lower in energy. Above T_C, the excitations outside the im-

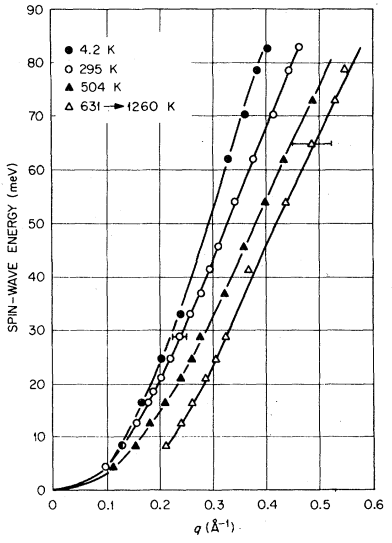

FIG. 2. Spin-wave dispersion relation for nickel at a series of temperatures. Above the transition temperature there is no change in the position of the scattering as observed in a constant-energy-transfer scan. The solid curves are the fits to Eq. (1) as discussed in the text.

mediate vicinity of $\Gamma(\vec{q}=0)$ persist up to the highest temperatures measured ($2T_C$), with no further renormalization of the spin-wave dispersion relations occurring. We have chosen to call this "spin-wave" scattering because of the continuous evolution of the scattering from low temperatures through T_C, and because we find that above T_C $\Delta E/E < 1$ at the higher energies. This behavior contrasts with that at small wave vectors where the spin waves become overcritically damped[11] just below T_C.

If the dispersion relation $E = Dq^2$ is fitted to the data in this energy range, then D is found to decrease from 550 meV Å^2 at 4.2 K to 280 meV Å^2 at and above T_C. It is interesting to note that at room temperature $D = 420$ meV Å^2, so that almost half the renormalization of the spin-wave energies at high energies occurs from $T/T_C = 0$ to $\sim\frac{1}{2}$, whereas the magnetization decreases by only $\sim 5\%$. If a higher-order term is included, viz.,

$$E = Dq^2(1-\beta q^2) \tag{1}$$

then at 4.2 and 295 K we obtain the values of $D = 593$ meV Å^2, $\beta = 0.68$ Å^2, and $D = 505$ meV Å^2, $\beta = 0.98$ Å^2, respectively. The room-temperature values are considerably different than the values obtained by Minkiewicz *et al.*[11] The reason for this difference is because for nickel the spin waves at small $\vec{q}$ lie lower in energy than this fitted dispersion relation would give, so that use of just the higher-energy data in the fitting procedure affects the fitted values considerably. It also emphasizes the dependence of D and β on one another. Direct comparison of the measured spin-wave energies where the two sets of data overlap show that the data themselves are in good agreement. We emphasize that these fits should be regarded simply as parameterizations of the spin-wave spectra and one should be cautioned against attributing much physical significance to D and β, especially at elevated temperatures. In fact Minkiewicz *et al.*[11] found it necessary to include terms in Eq. (1) out to q^{10} to obtain an adequate fit to the dispersion relation at room temperature over the range of wave vectors they explored.

Since the abrupt decrease of the spin-wave intensity at room temperature was found to occur at a considerably lower energy in the [111] direction than in the other symmetry directions,[19] detailed measurements of the temperature-dependent spin-wave intensities near the Stoner cutoff were taken only in the [111] direction. Figure 3 shows the intrinsic spin-wave intensity χ_s versus energy at a series of temperatures from 4.2 to 757 K ($1.2T_C$), where χ_s is obtained from the observed integrated intensity $I(E)$ by taking into account the thermal occupancy of the states and the density of states, viz.,

$$I_{\text{obs}}(E) \cong \frac{C(1+\langle n\rangle)\chi_s(E)}{|\vec{\nabla}_{\vec{q}}\omega|} . \tag{2}$$

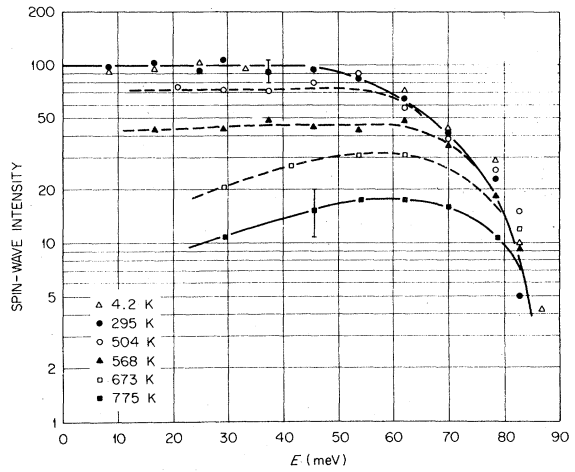

FIG. 3. Integrated intensity of the spin-wave (susceptibility) scattering as a function of energy and temperature for the [111] symmetry direction.

Here $\langle n\rangle$ is the thermal population factor, $1/\vec{\nabla}_{\vec{q}}\omega$ corrects for the density of spin-wave states at E (in a constant-E scan), and C is a constant relating the instrumental parameters. The interesting feature of χ_s is the rapid decrease which occurs at ~ 85 meV regardless of the temperature. The overall intensity decreases at higher temperatures (in a manner similar to iron), so that these measurements become increasingly more difficult. Since no change in the Stoner cutoff was observable as high as $1.2T_C$, and because of the very long counting times involved, accurate intensity measurements of the high-energy spin waves were not extended to higher temperatures. Although the temperature dependence of the spin-wave–Stoner-mode intersection was not measured in the other symmetry directions, measurements to 100 meV were taken both at 4.2 K and above T_C in the [100] direction to be certain that there was no qualitative difference in the behavior of the scattering in the other symmetry directions. The spin-wave intensities at room temperature are discussed in detail elsewhere.[13,14]

Another feature of the intensity data of Fig. 3 that deserves explanation is the decrease in χ_s at elevated temperatures at all energies. Part of this decrease in χ_s is due to a reduction in the observed intensity, below the expected value, and part is due to the temperature variation in the thermal occupation $\langle n\rangle$ [Eq. (2)]. The temperature dependence of $\langle n\rangle$ is of course largest at low energies, and this is what produces the "hump" in $\chi_s(E)$ at the highest temperatures; no such peak occurs in the raw integrated intensities. The temperature variation of the observed intensities at low energies is therefore considerably less rapid than might be inferred from Fig. 3. For comparison we note that in the case of a localized

spin system χ_s would be a constant value independent of temperature and energy, at least in the regime where linear spin-wave theory is valid.

An example of some spin-wave measurements at a series of temperatures above and below T_C is shown in Fig. 4. These data are for relatively high energy transfers and for $\vec{q}$ in the [111] direction. ζ is in reduced units and must be multiplied by $2\pi\sqrt{3}/a \simeq 3.08$ Å^{-1} to obtain values in Å^{-1}. Note that with increasing temperature the peaks shift to larger wave vector and broaden somewhat, but are easily observed above T_C. The solid curves are a least-squares fit to a Gaussian distribution plus background, and this is found to represent the spectra adequately at all temperatures. The sloping background in these higher-energy data is the result of scattering from the incident beam at these relatively small scattering angles, and was monitored by the background detector between the sample and analyzer. This background was also measured under identical conditions without the sample present.

Figure 5 shows the scattering for an energy transfer of 20.7 meV. At this lower energy considerably better resolution can be employed, which allows us to observe the temperature evolution of the scattering more closely. As the transition temperature (631 K) is approached from below the width of the spin-wave peak broadens, but above T_C little change is observed. Note also that the scattering is symmetric about the central position, and is again well represented by a Gaussian. We remark that at high

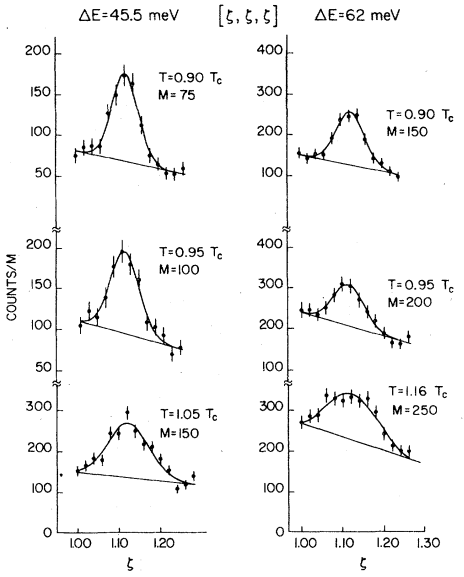

FIG. 4. Observed scattering at several temperatures above and below the Curie temperature for 45.5 and 62 meV. The solid curves are the least-squares fits to a Gaussian distribution plus background. $\zeta = 1.0$ corresponds to the Brillouin-zone center (111 reciprocal-lattice point).

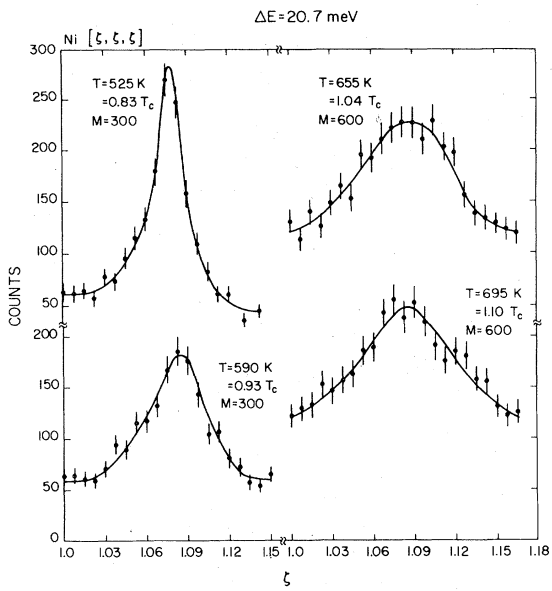

FIG. 5. Temperature evolution of the scattering at an energy transfer of 20.7 meV. With increasing temperature the scattering broadens and the centroid shifts to larger ζ (corresponding to renormalization of the spin-wave dispersion). Little additional change with temperature is found for $T \gtrsim T_C$.

temperatures the instrumental resolution in this case is small compared to the breadth of the scattering so that the observed shape is indicative of the intrinsic shape of the scattering function.

Figure 6 shows several scans above T_C for a still lower energy transfer of 12.41 meV around the 111 reciprocal-lattice point. Four peaks are clearly visible, two broad peaks due to the magnetic scattering at $\pm q$, and two narrow peaks due to the longitudinal phonons at $\pm q$. At room temperature there are four narrow well-resolved peaks, with the spin wave at $+q$ being twice as intense as the phonon at $+q$. (Above $\sim$20 meV the magnetic scattering is well separated from the phonons.) Note that the phonon intensity at $-q$ is considerably less than at $+q$. This is due to the fact that the cross section for phonon scattering is proportional to $|\vec{K}\cdot\hat{e}|^2$, where $\hat{e}$ is the (unit) polarization vector of the phonon. For this scan, $\vec{q}\|\vec{K}$, so that only the longitudinal ($\hat{e}\|\vec{q}$) phonon is visible. The measured integrated intensities of the phonons at $\pm q$ are related by the factor $|\vec{\tau} \pm \vec{q}|^2$. The spin-wave intensities at $\pm q$ differ through the variation of the magnetic form factor $F(\vec{K})$, so that the intensity of the magnon at $-q$ is somewhat greater than the one at $+q$. The solid curve in the figure is the computer least-squares fit of four Gaussian shaped peaks plus a linear background term as discussed in Ref. 14. The positions, widths, and intensities for $\pm q$ obtained from these fits are in good agreement with

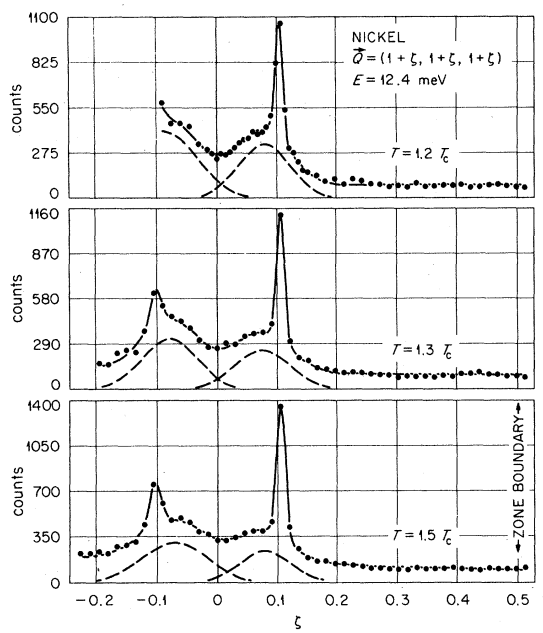

FIG. 6. Measured scattering above T_C around the 111 reciprocal-lattice point. The broad peaks at $\pm q$ are due to the magnetic scattering and the narrow peaks are due to the phonons. The solid curve is the least-squares fit to a sum of four Gaussian distributions plus background as described in the text. The intensity observed at larger $\vec{q}$ toward the zone boundary changes very little with temperature and is due to instrumental background.

each other once the appropriate variables in the cross sections and the resolution of the spectrometer are properly taken into account. As in the case of iron, there is no indication in these data of any interaction of the magnons with the phonons.

The scans in Fig. 6 have been extended to the Brillouin-zone boundary, and it is evident that there is no appreciable magnetic scattering other than the spin-wave scattering. Scans of this type have been carried out from room temperature up to $2T_C$, and from 4 to 29 meV. No scattering was observed other than the scattering due to the magnons and phonons. In particular we observed no significant temperature dependence to the scattering at large ζ (e.g., $\zeta > 0.3$) away from the magnetic and phonon scattering. At room temperature, for example, we observed 4.2 ± 0.3 counts/min background, originating primarily from fast neutrons, with a spin-wave signal-to-noise of 21 at 12.4 meV. At $T = 0.9T_C$ we observed 4.6 counts/min, and within statistics this did not change up to $2T_C$. We would like to emphasize that for the data below ~ 40 meV the background we have used to analyze the data is flat, and *temperature independent,* as was the case for iron.[16] The sloping background at higher energies is solely an instrumental effect due to the small scattering angles, and is also temperature independent in these data.

Several scans at 12.41 meV around the 111 reciprocal-lattice point are shown in Fig. 7 for temperatures up to $2T_C$. For clarity the data points which contain a significant phonon contribution have not been plotted. The magnetic scattering above T_C can be described in terms of two overlapping peaks centered at $\pm q$ which do not change position as a function of temperature, but slowly broaden. The peaks at $2T_C$ are in fact becoming quite broad, but are still easily discernible.

From the measurements of the magnetic scattering the linewidths in $\vec{q}$ may be extracted, and Fig. 8 shows the observed widths for an energy of 12.41 meV from liquid-helium temperature up to $2T_C$. The widths are seen to increase rapidly through the transition and continue to broaden slowly at the higher temperatures. This contrasts with the results for iron,[16] where no further increase in the widths above T_C was observed. An estimate of the energy width can be obtained from

$$\Delta E = |\vec{\nabla}_{\vec{q}}\omega|\Delta q \ , \qquad (3)$$

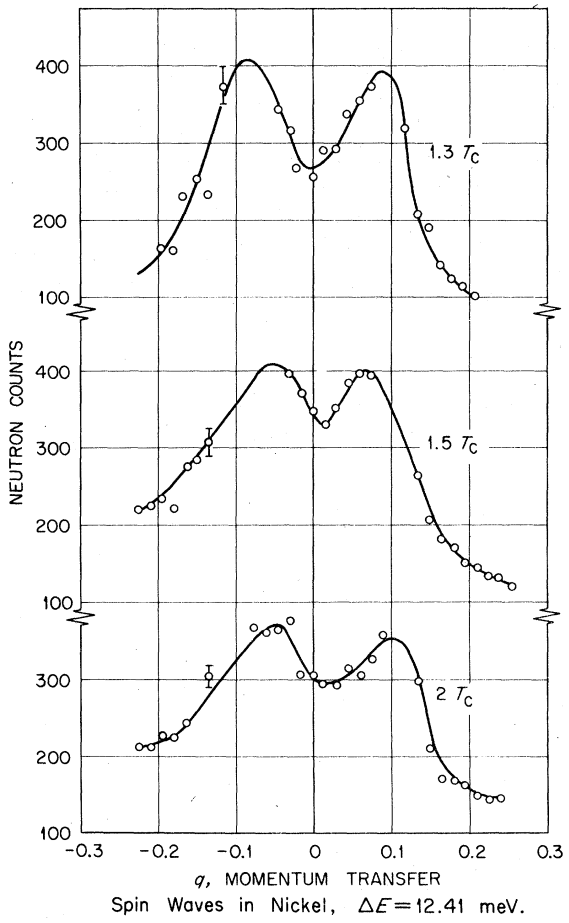

FIG. 7. Magnetic scattering at $\pm q$ for 12.41 meV covering temperatures up to $2T_C$.

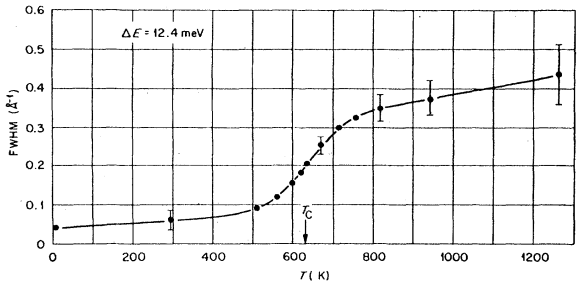

FIG. 8. Observed linewidths of the magnetic scattering as a function of temperature for 12.41 meV. The width at $T = 4.2$ K is due to the resolution of the spectrometer.

where $\vec{\nabla}_q \omega$ is the slope of the dispersion relation and Δq is the observed width (e.g., half-width at half maximum) in $\vec{q}$. Then at T_C we find $\Delta E/E \simeq 0.9$. As the linewidth increases, $\Delta E/E$ becomes greater than one, so that in this sense the concept of a spin wave certainly becomes ill defined at this energy. At $2T_C$, $\Delta E/E \simeq 1.9$.

Figure 9 shows the linewidths for an energy transfer of 24.8 meV. The general behavior is the same as for 12.41 meV, except that the rate of increase of the linewidths is slower just after T_C, instead of continuing to increase fairly rapidly above T_C. (For 12.41 meV, $\Delta E/E > 1$ before the rate of increase slows.) At T_C, $\Delta E/E \simeq 0.8$, and at $2T_C$, $\Delta E/E \simeq 1.2$. Note that at a fixed temperature above T_C, $\Delta E/E$ is smaller for the higher energy, and in general $\Delta E/E$ was found to decrease with increasing energy. The experimental results indicate that above an energy transfer of ~ 35 meV, $\Delta E/E < 1$ up to the highest temperature measured ($2T_C$).

In comparing the experimental measurements of Fe and Ni, it should be noted that in general the measurements on nickel were more difficult to carry out for several reasons. First, the Fe sample was somewhat larger, and the magnetic moment is about four times greater so that the magnetic scattering was considerably stronger from the Fe sample. The spin-wave dispersion relations are also steeper in nickel, so that the spin-wave scattering in a constant energy transfer scan is reduced. In addition, because of the steepness of the dispersion surface, the spin waves at $\pm q$ in Ni begin to overlap at the higher temperatures, so that they must both be measured in order to separate the contributions from one another. The resolution of the spectrometer also becomes more important, and considerably better resolution had to be employed for the lower-energy measurements in nickel compared with iron. Improving the resolution reduces the observed scattering intensity, and hence increases the experimental running time. For iron the magnetic inelastic scattering at $\pm q$ did not overlap appreciably even at an energy transfer as small as 8 meV. The steep dispersion for the scattering in nickel is also what makes it impossible (at present) to measure the scattering at fixed momentum transfer. A constant-$\vec{Q}$ scan would be preferable to extract the spin-wave linewidths, and in particular to demonstrate more directly the propagating character of the scattering at high energies— large wave vectors for $T > T_C$. The results for iron demonstrated, however, that Eq. (3) does yield accurate values for the energy widths, and the essential point is that we find for nickel that $\Delta E/E < 1$ at the higher energies. We can also state that at the larger wave vectors the scattering intensity *increases* with increasing energy, so there is by necessity a peak at finite energy above T_C. The scattering is too steep, however, to allow a measurement of the complete peak, that is, to observe the decrease of the intensity at high energies. This could be done in the case of iron[16] since the scattering there is considerably less dispersive.

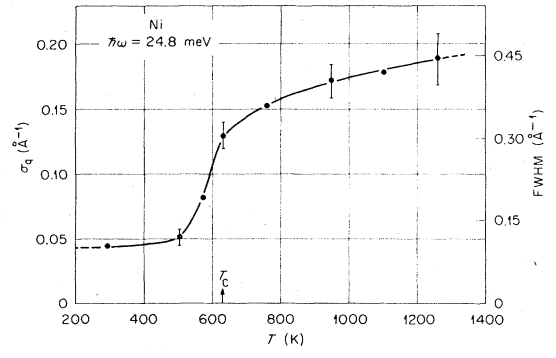

FIG. 9. Observed linewidths vs temperature for 24.8 meV. σ_q is defined in terms of the standard deviation of a Gaussian distribution.

IV. DISCUSSION

The results for nickel and iron demonstrate that the scattering above the magnetic phase transition has a propagating spin-wave-like character outside the small-wave-vector—low-energy region. This type of behavior has been observed[20,21] in lower-dimensional systems where the long-wavelength fluctuations suppress the transition, but it was not anticipated in magnetically isotropic three-dimensional systems such as nickel and iron. Similar behavior has recently been observed in other transition-metal systems[22–24] and in Gd.[25]

In the small wave-vector region the scattering in nickel was found by Minkiewicz *et al.*[11,26] to be in general agreement with hydrodynamic theory,[27] and our data at small $\vec{q}$ are in good agreement with their data. With increasing energy (and wave vector), however, the scattering progressively departs from the hydrodynamic predictions until at high energies it

is in qualitative disagreement. For example a simple form for the scattering function $S(q,\omega)$ above T_C in the hydrodynamic regime is

$$S(\vec{q},\omega)=\frac{1}{q^2+\kappa^2}\frac{\Lambda q^2}{(\Lambda q^2)^2+\omega^2}\ , \tag{4}$$

where κ is the inverse correlation length and Λ is the spin-diffusion constant. For a fixed energy transfer (i.e., fixed ω), we note that

$$\begin{aligned} &S(0,\omega)=0\ , \\ &\lim_{q\to\infty} S(\vec{q},\omega)\propto\frac{1}{q^4}\to 0\ , \end{aligned} \tag{5}$$

so that there will obviously be a peak in the predicted scattering at some finite q. However, for the measured parameters of Ni Eq. (4) predicts a very broad peak which is distinctly asymmetric at high energies, whereas the observed scattering has a width which is $\sim\frac{1}{5}$ of that calculated, and is symmetric in shape. The intrinsic shape of the scattering as a function of $\vec{q}$ is in fact well represented by a Gaussian function. We also tried to fit a Lorentzian-shaped scattering function (convoluted with the instrumental resolution) to the observed scattering but this did not adequately represent the data.

We remark that the scattering expected for a weak itinerant ferromagnet above T_C, i.e., the Pauli paramagnet, in no way resembles the magnetic scattering observed in Ni. This Pauli scattering can be very easily calculated by evaluating the Stoner density of states with the band splitting set to zero (see Ref. 2). The magnetic excitations in this case are spread over an energy of the order of the bandwidth (i.e., $\sim$ several eV). Of course this type of calculation neglects the electron-spin correlations above T_C, whereas we know that the inclusion of these correlations is absolutely essential to understanding the spin dynamics of these band ferromagnets at any temperature. Our experiments demonstrate that the nature of the magnetic state above T_C more closely resembles the ground state than the Pauli paramagnetic state. The task of theory is then to properly incorporate these spin correlations—a formidable job even at $T=0$.[1-3] Nevertheless considerable progress has been made.[4-10] With regard to the present experiments we remark that the theory of Korenman and Prange[6,28] predicts a line shape and temperature dependence to the widths which are in agreement with experiment.

The scattering in nickel has also been compared with the quasi-spin model of Liu.[4] Unfortunately the comparison[4] was made to data whose widths were dominated by instrumental resolution, and the intrinsic widths as determined by high-resolution measurements are considerably narrower than this. In addition, the instrumental background, which is essentially independent of temperature, was considered to originate from multimagnon contributions to the theoretical cross section. Under the circumstances no conclusions can be drawn from the comparison.

Finally we remark that no scattering was observed other than that due to the magnetic scattering and to phonons. In particular we found no evidence of any "mixed modes" as has been reported by Frikkee.[29] To search for this scattering additional measurements were carried out on a ^{58}Ni single crystal as well as a single crystal with the natural distribution of isotopes. Our conclusion is that the scattering reported[29] is most likely due to incoherent phonon scattering. Further details can be found in Ref. 30.

V. SUMMARY

The inelastic scattering of neutrons has been used to measure the spin dynamics of nickel from low temperatures to twice the ferromagnetic transition temperature. In contrast to the behavior observed in the small-wave-vector region, where the spin waves were found to become overcritically damped just below T_C, we find that the scattering at larger wave vectors can be described in terms of propagating excitations up to the highest temperatures measured. The dispersion relation for these higher-energy excitations as measured in a constant-energy-transfer scan is only moderately renormalized up to T_C and then remains constant as the temperature is increased further. Measurements of the intrinsic linewidths show that the spin waves do broaden considerably as the temperature is raised to T_C, but do not become overcritically damped at the higher energies. Above T_C the widths continue to increase slowly, in contrast to iron where there is no appreciable change in the widths above T_C. The intrinsic shape of the scattering as a function of wave vector is well represented by a Gaussian.

The overall strength of the susceptibility is reduced at higher temperatures, but the abrupt decrease in magnitude at high energies, interpreted as due to the region of high density of Stoner excitations, is found to be insensitive to the temperature. Aside from this spin-wave–Stoner-mode intersection, the dynamic susceptibility $\chi(\vec{q},\omega)$ is isotropic in $\vec{q}$ over the entire temperature and energy ranged explored. No interaction of the spin waves with the phonons was observed, and no evidence of inelastic scattering other than that due to spin waves and phonons was found.

ACKNOWLEDGMENTS

We would like to thank J. F. Cooke, H. L. Davis, H. A. Gersch, C. J. Glinka, T. Kaplan, V. Korenman, R. M. Nicklow, R. E. Prange, and M. K. Wilkinson for very helpful discussions and assistance. Research was sponsored by the U.S. Department of Energy under Contract No. W-7405-ENG-26 with the Union Carbide Corporation.

*Oak Ridge Associated Universities participant from the Georgia Institute of Technology. Portions of this work are taken from a Ph.D. thesis submittted to the Georgia Institute of Technology.

†Permanent address: Department of Physics, University of Maryland, College Park, Md. 20742.

[1]J. F. Cooke and H. L. Davis, in *Magnetism and Magnetic Materials—1972,* edited by C. D. Graham and J. J. Rhyne, AIP Conf. Proc. No. 10 (AIP, New York, 1973), p. 1218.

[2]J. F. Cooke, J. W. Lynn, and H. L. Davis, Solid State Commun. 20, 799 (1976); *Magnetism and Magnetic Materials—1974,* edited by C. D. Graham, G. H. Lander, and J. J. Rhyne, AIP Conf. Proc. No. 24 (AIP, New York, 1975), p. 329; Phys. Rev. B 21, 4118 (1980).

[3]J. F. Cooke, Phys. Rev. B 7, 1108 (1973).

[4]S. H. Liu, Phys. Rev. B 13, 2979, 3962 (1976); 15, 4281 (1977); 17, 3629 (1978).

[5]J. B. Sokoloff, Phys. Rev. Lett. 31, 1417 (1974); J. Phys. F 5, 528, 1946 (1975); Phys. Rev. B 13, 4172 (1976); 17, 2380 (1978).

[6]V. Korenman, J. L. Murray, and R. E. Prange, Phys. Rev. B 16, 4032, 4048, 4058 (1977).

[7]T. Moriya, J. Phys. Soc. Jpn. 40, 933 (1976); T. Moriya and Y. Takahashi, *ibid.* 45, 397 (1978).

[8]D. M. Edwards, J. Phys. F 6, L289 (1976).

[9]M. A. Klenin and J. A. Hertz, in *Magnetism and Magnetic Materials—1975,* edited by J. J. Becker, G. H. Lander, and J. J. Rhyne, AIP Conf. Proc. No. 29 (AIP, New York, 1976), p. 270.

[10]J. Hubbard, Phys. Rev. B 19, 2626 (1979); 20, 4584 (1979).

[11]V. J. Minkiewicz, M. F. Collins, R. Nathans, and G. Shirane, Phys. Rev. 182, 624 (1969).

[12]R. D. Lowde and C. G. Windsor, Adv. Phys. 19, 813 (1970).

[13]H. A. Mook, R. M. Nicklow, E. D. Thompson, and M. K. Wilkinson, J. Appl. Phys. 40, 1450 (1969); H. A. Mook, J. W. Lynn, and R. M. Nicklow, in *Magnetism and Magnetic Materials—1973,* edited by C. D. Graham and J. J. Rhyne, AIP Conf. Proc. No. 18 (AIP, New York, 1974), p. 781.

[14]H. A. Mook, Phys. Rev. Lett. 43, 2029 (1979).

[15]H. A. Mook and R. M. Nicklow, Phys. Rev. B 7, 336 (1973).

[16]J. W. Lynn, Phys. Rev. B 11, 2624 (1975).

[17]H. A. Mook, J. W. Lynn, and R. M. Nicklow, Phys. Rev. Lett. 30, 556 (1973).

[18]M. J. Cooper and R. Nathans, Acta Crystallogr. 23, 357 (1967); B. N. Brockhouse, L. N. Becka, K. R. Rao, and A. D. B. Woods, *Second Symposium on Inelastic Scattering of Neutrons in Solids and Liquids* (IAEA, Vienna, 1963), Vol. II, p. 23.

[19]Higher-intensity measurements (Ref. 14) show that the spin-wave scattering persists to higher energies, but is reduced in overall intensity by more than an order of magnitude.

[20]M. T. Hutchings, G. Shirane, R. J. Birgeneau, and S. L. Holt, Phys. Rev. B 5, 1999 (1972); Y. Endoh, G. Shirane, R. J. Birgeneau, P. M. Richards, and S. L. Holt, Phys. Rev. Lett. 32, 170 (1974); G. Shirane and R. J. Birgeneau, Physica (Utrecht) 87, 639 (1977).

[21]M. Steiner, B. Dorner, and J. Villain, J. Phys. C 8, 165 (1975); M. Steiner, J. Villain, and C. G. Windsor, Adv. Phys. 25, 87 (1976).

[22]K. Mikke, J. Jankowska, and A. Modrzejewski, J. Phys. F 3, L173 (1973); Phys. Status Solidi B 59, K97 (1973).

[23]T. M. Holden, J. Phys. F 6, 433 (1976).

[24]Y. Ishikawa, G. Shirane, J. A. Tarvin, and M. Kohgi, Phys. Rev. B 16, 4956 (1977); J. A. Tarvin, G. Shirane, Y. Endoh, and Y. Ishikawa, Phys. Rev. B 18, 4815 (1978).

[25]R. M. Nicklow (private communication).

[26]V. J. Minkiewicz, Int. J. Magn. 1, 149 (1971).

[27]B. I. Halperin and P. C. Hohenberg, Phys. Rev. 177, 952 (1969).

[28]V. Korenman and R. E. Prange, Solid State Commun. 31, 909 (1979); R. E. Prange and V. Korenman, Inst. Phys. Conf. Ser. 39, 567 (1978).

[29]E. Frikkee, Phys. Lett. 34A, 23 (1971); Reactor Centrum Nederland (Petten) Report No. 185 (1973) (unpublished).

[30]J. W. Lynn, Ph.D. thesis (Georgia Institute of Technology, 1974) (unpublished).